

中央研究院
資訊科學研究所

Institute of Information Science, Academia Sinica • Taipei, Taiwan, ROC

TR-IIS-07-003

Exact Collision Detection for Scaled Convex Polyhedral Objects

Jing-Sin Liu, Y.H. Tsao, Wen-Yang Ku, Wen-Hwa Pan and Y.-Z. Chang



January 19, 2007 || Technical Report No. TR-IIS-07-003

<http://www.iis.sinica.edu.tw/LIB/TechReport/tr2007/tr07.html>

Exact Collision Detection for Scaled Convex Polyhedral Objects

Jing-Sin Liu*, Y.H. Tsao**, Wen-Yang Ku*

*Institute of Information Science
Academia Sinica
Nankang, Taipei 115, Taiwan, R.O.C
liu@iis.sinica.edu.tw

Wen-Hwa Pan* and Y.-Z. Chang**

**Department of Mechanical Engineering
Chang Gung University
Tao-Yuan, Taiwan, R.O.C

Abstract – This paper addresses the following collision detection problem: determine the collision status for a pair of stationary convex polyhedral objects whose allowed deformation is uniform but arbitrary scaling of vertices within given upper and lower limits. We present an exact overlap checking method based on the characterization of all contact configurations. The set of all scaling pairs that two objects contact each other externally is characterized by a descending piecewise linear curve where the switching point of this piecewise linear curve represents the scaling pair as long as the contact configuration changes feature. Then, using this piecewise linear curve, the rectangle of allowable scaling pairs is partitioned into an exact overlap and an exact non-overlap sub-regions. A corresponding decision curve for exact overlap checking is constructed from this scaling decision curve via parametric intersection points of each polyhedron with the shortest path between inner ellipsoids of deformation bounds.

Index Terms - collision detection, convex polyhedra, deformation, scaling

I. INTRODUCTION

COLLISION detection [1], [5] is the process of finding the geometrical or physical contacts between the (static or moving, rigid or deformable) objects. A wealth of existing works on solving the broad and narrow phases of collision detection problems, either approximate or exact, is developed for rigid convex polyhedra and some for arbitrary polyhedra (see the survey for virtual environments or graphics [1], [2], [10], or the survey in robot motion planning [16]). A numerical approach to approximate collision detection of convex polyhedral objects based on inner ellipsoids has been developed in recent years [3], in contrast to the approach via outer ellipsoids [9],[11]. Overlap between convex polyhedra can be detected via the intersection points of convex polyhedra with the shortest path between inner ellipsoids, where tradeoff among accuracy, efficiency, memory storage and user control of these factors was demonstrated in the performed experiments.

Recently there are increasing interests in collision detection for deformable objects (see [12] for a state of the art report in the graphics community) undergoing different types of deformation [5]-[9]. The shape and topology of the object may change during certain types of deformation which would complicate the collision detection process for deformable objects. Very few methods that perform well for collision detection of rigid objects can also be extended to be applied on objects undergoing different type of geometric or physical deformations [6]-[9]. Among the methods, bounding volumes hierarchies (BVHs) are widely applied on a variety of deformation models, either alone or combined with other methods (e.g. hash-table, sweep and prune) [12] to trade accuracy for speed. Some obvious drawbacks of BVHs updating approach are: (i)BVHs can drastically change during deformation. Only the primitives like sphere-trees whose overlap checking is easy are of practical use [6], [9]. (ii) complete rework on the bounding volumes for constantly changing shape and topology of the objects at each time step of deformation is a time-consuming process and thus usually is very slow.

To speed-up the refitting process, partial refitting of BVHs are applied to localize “interesting regions”, which are later stochastically sampled to elaborate the search for (local) closest features [12]. BVH has been applied to collision detection of convex polyhedral objects with arbitrary vertex repositioning [5]. This paper studies the exact collision detection of convex polyhedral objects undergoing scaling transformation (uniform vertex repositioning, i.e. scaling the size of the objects while shapes remain unchanged) employing the shortest path between inner ellipsoids [4]. The scaling transformation is important as an elementary operation of affine transformation [1]. The growth distance [20] is defined via identical scaling of a pair of convex

polyhedra. Scaling can also be used in producing an exaggeration effect on entire motion clips or gated segments of clips of captured human motion data [24]. In general, the collision status of a pair of scaled convex polyhedral objects can be detected exactly (i.e. no collisions may occur without being detected) by repeatedly applying the method of (enhanced) GJK [1], [22] at each scaling timeframe. By contrast, this paper develops an exact collision detection for uniformly scaled convex polyhedra via reference to a descending piecewise linear decision curve characterizing the set of all contact configurations. Furthermore, in contrast with the GJK approach based on the closest points (see e.g. [1], [5]), the proposed *exact* collision detection approach is based on the decision curve constructed on the plane of parametrized *estimated* closest points in the direction of shortest path between inner ellipsoids. It has recently been found that the signed distance along a given direction (i.e. directional distance) can be used to efficiently detect the overlapping of two convex polyhedra and compute their corresponding penetration depth (PD) for overlapping pairs of objects [1], [15], [18]-[20] which is defined as the minimum translational distance over which one object needs to be displaced in order to bring two overlapping objects into touching contact [20], [1]. Usually the Minkowski sum of two polyhedra and Gauss map are employed to develop algorithms for computation of PD or its estimate, which is used to generate visually acceptable collision response of overlapping. Also, one can define other measures, for example, pseudo-distance [21] as a unified distance metric for two objects that are separating or intersecting.

The paper is organized as follows. Piecewise linear curve characterizing the set of all touching scalings of two scaled convex polyhedra is introduced in Section II. In Section III, we proceed to exact collision detection based on the piecewise linear curve characterizing all contact configuration of objects. Finally, we conclude this paper in Section IV.

II. Piecewise linear relationship between touching scalings

2.1. Deformation model: Uniform scaling

For each convex polyhedron, the uniform deformation of vertex coordinates assumes that any point on the object undergoes the same fraction of stretching or compressing displacement relative to an interior point, called seedpoint s_i so that

$$\tilde{p}_i = \rho_i p_i$$

where $\tilde{p}_i = (\tilde{x}_i, \tilde{y}_i, \tilde{z}_i) - s_i$ is the displacement of a point $p_i = (x_i, y_i, z_i) - s_i$ undergoing a scaling transformation ρ_i of each polyhedral object [20]. Throughout this paper, $(P_1(\rho_1), P_2(\rho_2))$ denotes the pair of objects after applying the scaling pair (ρ_1, ρ_2) to the object pair (P_1, P_2) . For brevity, the configuration of $(P_1(\rho_1), P_2(\rho_2))$ is also represented uniquely and interchangeably by the scaling pair (ρ_1, ρ_2) .

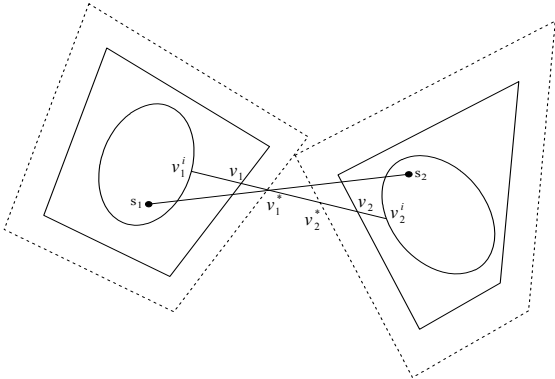


Fig. 1 Two scaled convex polyhedra with inner ellipsoidal deformation bounds are in external touch.

2.2. Shortest path between inner ellipsoids

Consider two undeformed convex polyhedra, P_1 and P_2 with known configuration. To determine the overlap status of the pair of scaled convex polyhedra $(P_1(\rho_1), P_2(\rho_2))$ for different scaling pair (ρ_1, ρ_2) , we first construct an inner ellipsoid E_1^i, E_2^i respectively for each object as inner deformation bounds (Fig. 1) [3]-[4]. Let the closest points between inner ellipsoids E_1^i, E_2^i be v_1^i and v_2^i , respectively. The point at which the ray emanating from v_1^i (respectively, v_2^i) toward v_2^i (respectively, v_1^i)

(respectively, v_1^i) intersects the boundary of $P_1(\rho_1)$ (respectively, $P_2(\rho_2)$) is denoted as v_1 (respectively v_2). The intersections are parametrized respectively as

$$\begin{aligned} v_1(\rho_1) &= v_1^i + t_1(\rho_1)(v_2^i - v_1^i), t_1 \in [0,1] \\ v_2(\rho_2) &= v_2^i - t_2(\rho_2)(v_2^i - v_1^i), t_2 \in [0,1] \end{aligned} \quad (1)$$

2.2.1 Touching scaling pairs

A pair of objects P_1, P_2 contact each other externally if

$$\text{int}(P_1) \cap \text{int}(P_2) = \text{empty set}$$

where int denotes the interior of the polyhedron. A touching scaling pair is (ρ_1, ρ_2) such that $(P_1(\rho_1), P_2(\rho_2))$ contact externally. In addition, the intersections of shortest path along the inner ellipsoids with $(P_1(\rho_1), P_2(\rho_2))$ assuming in contact configurations can be parametrized as (Fig. 1)

$$v_1 = v_1^i + t_1(v_2^i - v_1^i), v_2 = v_2^i - t_2(v_2^i - v_1^i)$$

Note that the contact configuration/scaling is unique for identically scaled convex polyhedral objects, while there are infinitely many contact configurations/scaling pairs for uniformly non-identically scaled convex polyhedral objects. A contact configuration of two convex objects is represented by the contact feature pair, whose features may change for different contact configurations. As the scaling applied to deform each convex polyhedral object is uniform but not identical, the exact overlapping conditions are more involved due to: (i) there are infinitely many contact configuration between scaled polyhedra, and (ii) the contact features may be varied for different contact configurations.

Consider a pair of stationary convex polyhedral objects at an initially underformed configuration, its configuration undergoing scaling transformation can be represented by their scaling pair. If (ρ_1, ρ_2) dominates (μ_1, μ_2) , i.e. ρ_i is not less than μ_i , $i=1,2$, and at least one ρ_i is larger than μ_i , the objects in configuration (ρ_1, ρ_2) are getting closer than in configuration (μ_1, μ_2) measured in the direction of the shortest path of inner ellipsoids, which is smaller if the objects are apart (or penetrating deeper if the objects are overlapping). Thus to detect the overlap status of a configuration represented by (ρ_1, ρ_2) , it can be approached from the characterization of all contact configurations which separate the overlap and non-overlap situations. If (ρ_1, ρ_2) dominates the contact configurations (ρ_1^*, ρ_2) or (ρ_1, ρ_2^*) as one object is fixed, then the pair of objects is overlapping; else, non-overlap is reported.

2.3 Characterization of the set of all touching scaling pairs

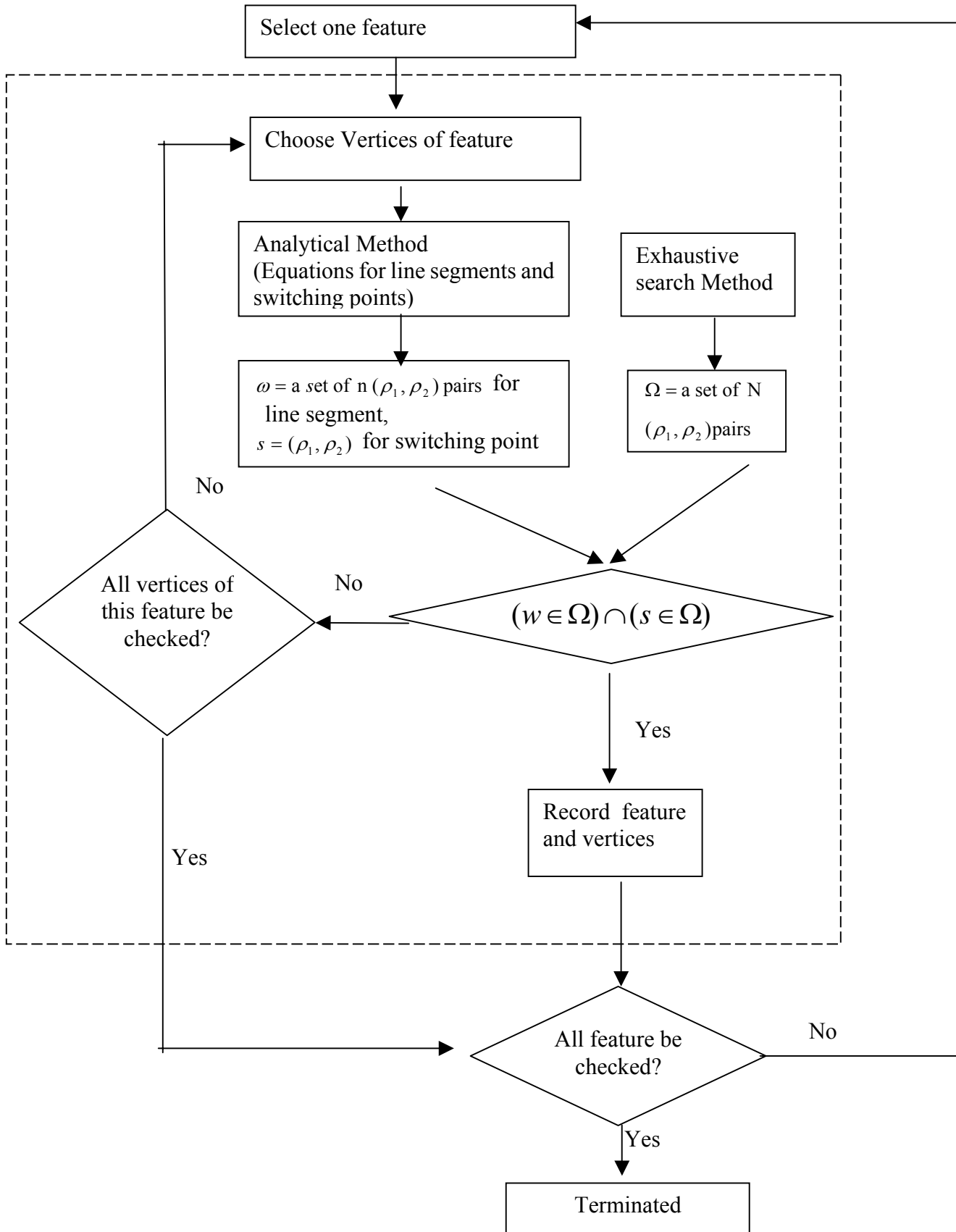
2.3.1 Piecewise-linear relationship between touching scaling pairs

A touching contact between two convex polyhedra, which has six variants (as illustrated in Fig. 6 in Appendix), can be represented by the feature pair, one feature from each object. These can be further reduced as three basic contacts expressed as face-vertex (F,V), edge-edge (E,E) or vertex-edge (V,E) contact. In any of the six contact types, the set of touching scaling pairs (ρ_1, ρ_2) respects a linear relationship (see Appendix for analytical derivations)

$$\rho_2 = a\rho_1 + b, a < 0 \quad (2)$$

That is, for a contact configuration (P_1, P_2) , if P_1 is scaled by ρ_1 then P_2 should be scaled by ρ_2 via (2) to maintain external contact without change in contact features. As (ρ_1, ρ_2) varies over all of the allowable ranges, denoted by $I_1 \times I_2$, a descending piecewise linear curve can be constructed by putting together each segment described by (2) for each contact feature, and the junction (switching point) is the scaling pair for which the contact feature changes.

Fig.2 Flowchart for computing all line segments that characterize the set of all touching scaling pairs.



2.3.2 Computation of the piecewise linear curve

Fig. 2 is a computational scheme for construction of the descending piecewise linear curve characterizing the set of all touching scaling pairs, mainly through exhaustive search of touching scaling pairs within the allowable ranges from scratch. Choosing a resolution for (ρ_1, ρ_2) amounts to discretize the rectangle $I_1 \times I_2$ into rectangular grid, where each node represents a configuration. By exhaustive search, a sufficient number of nodes corresponding to touching scaling pairs is found for construction of the piecewise linear curve characterizing the the set of all touching scaling pairs over $I_1 \times I_2$. This search for contact configurations over the grid representation of the rectangle $I_1 \times I_2$ is an expensive, lengthy process. There are two obvious drawbacks of using only exhaustive search in the construction of the descending piecewise linear curve that can introduce errors in practical applications: (i)The junction between adjacent line segments will be likely missed if the resolutions are not fine enough, and the junction is not sampled in the search process, (ii)For two adjacent line segments with nearly the same slopes, they are often not distinguishable and will be pieced together as one line segment so that contact feature change is missed at all. To overcome the drawbacks, the analytical equations derived in Appendix are invoked to aid for correct construction and reduce the computational expenses of exhaustive search.

Using the analytical equations to calculate the line segments and the junctions, if the contact features and vertices of feature are correct, the line segments from analytical equations will be the same with the results of exhaustive search, and easier to distinguish even the two line segments looks very closely because the slopes are more accurate(Fig. 3). Otherwise, the junctions will be the exact ones, don't need to consider about the resolution of sampling(Fig. 4).

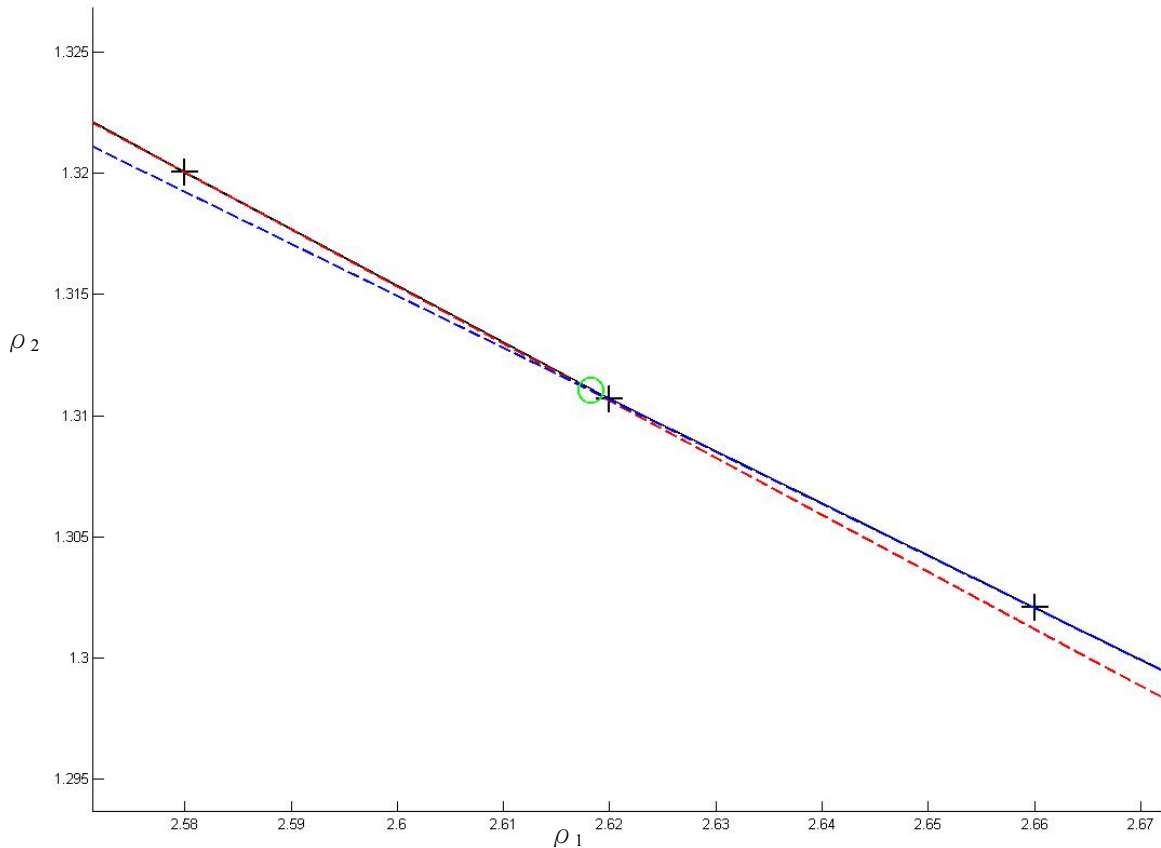


Fig. 3 . Black + : exhaustive search results. Blue -- and Red -- : results of analytical equations. Circle : junction of analytical equations.

It's easy to distinguish the two line segments from the analytical equations results.

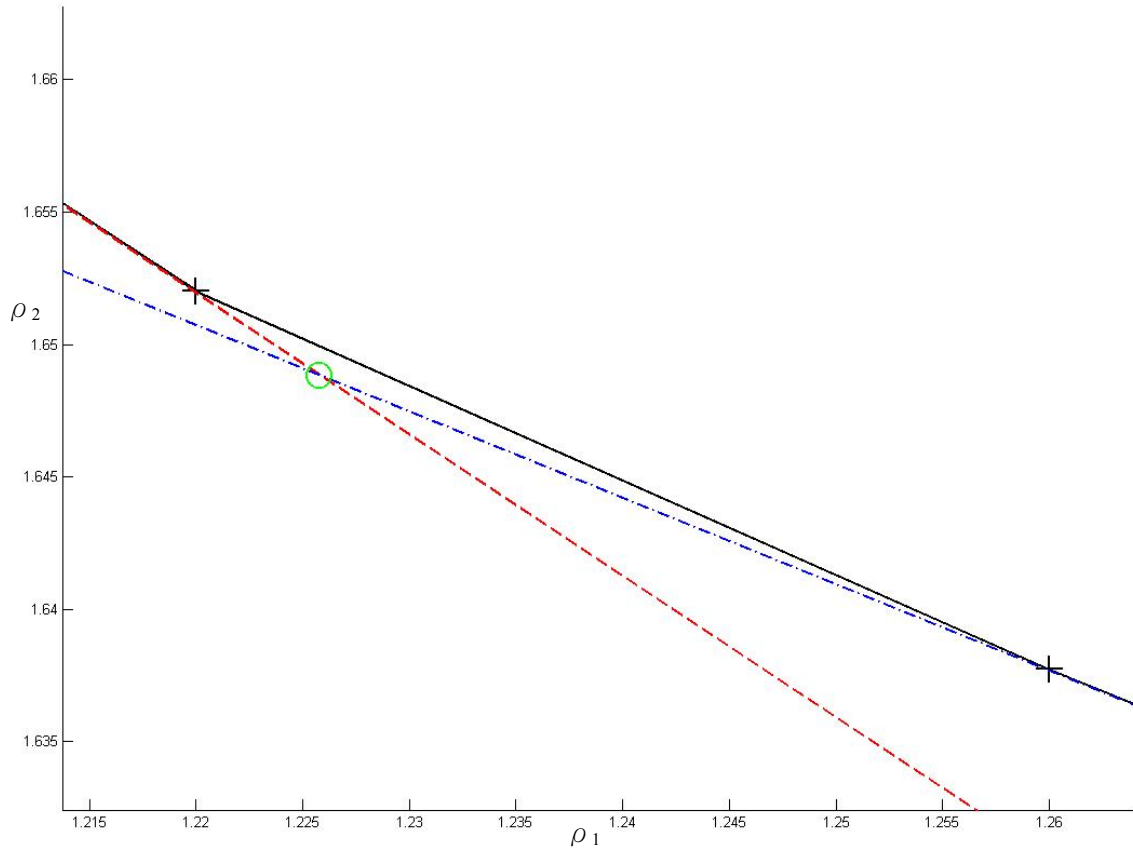


Fig. 4 . Black + : exhaustive search results. Blue -- and Red -- : results of analytical equations. Circle : junction of analytical equations.

Exhaustive search could not find out the exact junction because the resolution of sampling is not fine enough. But using analytical equations could get the exact junction.

In particular, the intersection of this curve with the line $\rho_2 = \rho_1$ is the growth distance [20], in the form of $\rho^* = b/(1-a)$.

In addition, this linear relationship implies that the contact loci is also a decending piecewise linear curve which switches from a line segment to another line segment with flatter negative tangent as contact feature changes. The contact features (V,E), (E,F) are generic transitions between two consecutive contacts (V,F) and non collinear (E,E) contacts [22]. (V,E) contact very often acts as the switching point of contact feature changes. Fig.5 shows an example of contact features transition as the touching scaling pair is varied over a given range, where we observe that, as the contact features change, the linear relationship between $\rho_1 - \rho_2$ for contact configurations is also changed.

III. Exact collision detection via decision curve

By mapping (2) from (ρ_1, ρ_2) plane to $t_1 - t_2$ plane, a piecewise linear decision curve of $t_1 - t_2$ is constructed for checking the collision status of scaled convex polyhedra.

3.1 Procedure for Exact collision detection

Now we summarize the procedure for checking the overlap of two scaled convex polyhedra via t_1, t_2 .

Given:

(i) two scalable convex polyhedra P_1, P_2 in an initially undeformed configuration, and their allowable scaling range $(\rho_1, \rho_2) \in I_1 \times I_2$ with respect to the seedpoints S_1, S_2 .

(ii) a configuration $P_1(\rho_1), P_2(\rho_2)$ to be checked for overlapping

Procedure:

Step 1(construction of overlap decision curve) Determine the descending piecewise linear curve of touching scaling pairs (Flowchart Fig.2).

Step 2. (Select a direction to estimate closest points between the objects). Calculate the shortest path between inner ellipsoids. As an alternative, the shortest path can be replaced by an arbitrary line segment with endpoints well inside the scaled convex polyhedra (e.g. the seedpoints).

Step 3. Compute the corresponding piecewise linear curve in the triangle $\{(t_1, t_2) : (t_1, t_2) \in [0,1]^2, t_1 + t_2 \leq 1\}$ of parametrized estimated closest points of $P_1(\rho_1), P_2(\rho_2)$ in the direction selected in Step 2.

Step 4. Compute (t_1, t_2) for current configuration.

Output: Report overlap/non-overlap of $P_1(\rho_1), P_2(\rho_2)$.

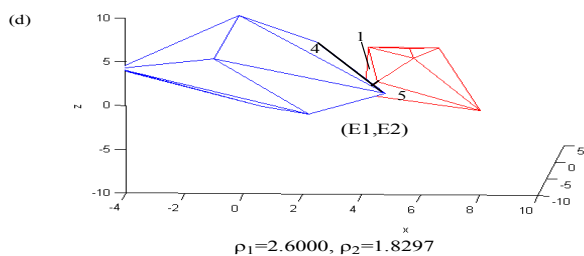
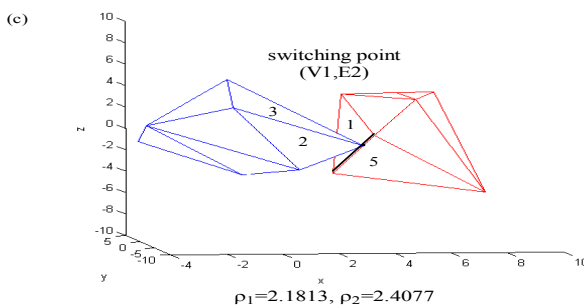
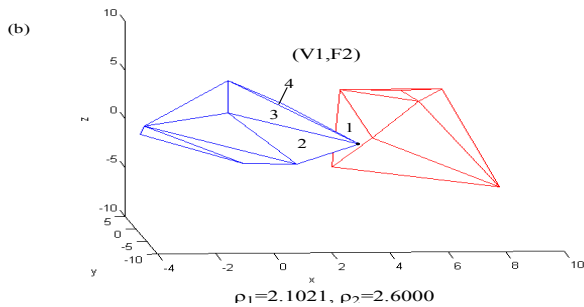
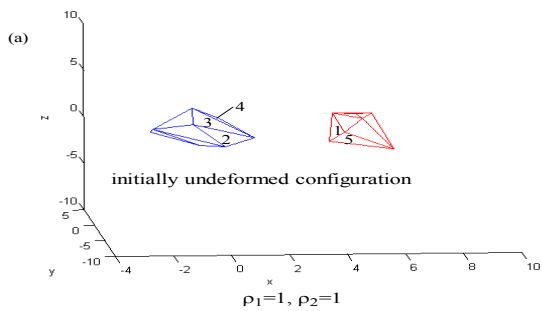


Fig.5 Contact features may change as the touching scaling pairs vary. This figure shows the changes of contact feature: (from top to bottom) undeformed configuration, contact feature (V1,F2), switching feature (V1,E2), contact feature (E1,E2). The seedpoint is the centroid (i.e. arithmetic average of vertices) of each polyhedral object.

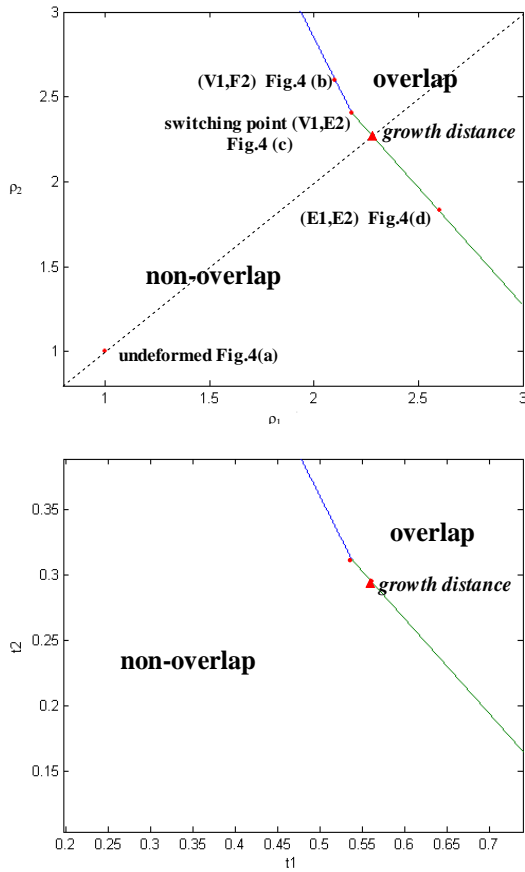


Fig. 6 Fig.5 continued: the diagrams that quantifies the descending piecewise linear relationship of contact configurations for $(\rho_1, \rho_2) \in [0.8, 3]^2$ and for $t_1 - t_2$.

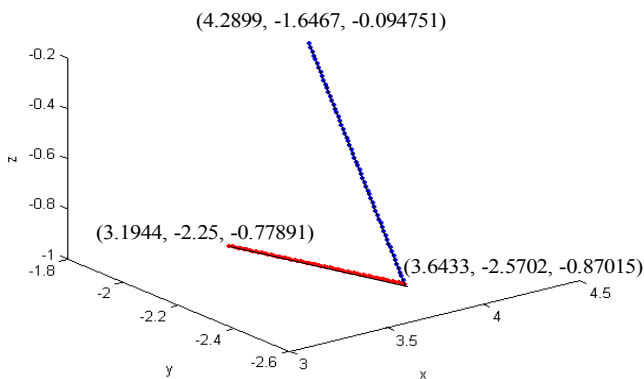


Fig.7 The piecewise linear loci of contact points of Fig.5.

3.2 Computational issues

For implementation, we search for the collision pair using a fast triangle intersection check [1] by triangulating the faces of each scaled polyhedral object. Except for the trivial situations that the objects are overlapping /non-overlapping over all ranges of scaling, one touching scaling (ρ_1^*, ρ_2^*) within the rectangle $I_1 \times I_2$ of allowable scaling can be computed by a bisection search

between a penetration situation and a separation situation. To reduce the numerical inaccuracy due to roundoff errors, the bisection method can be run a couple of times and their average is the outcome of the bisection search. To generate the piecewise linear curve characterizing the set of all touching scalings and the loci of contact points, the procedure is given in the flowchart of Fig. 2. As an example, Fig.6 shows the piecewise linear plot of all touching scalings, growth distance and the parametrized intersection points of $\overline{s_1 s_2}$ with scaled polyhedra for Fig.3, and the negative tangent is flatter after switching. Fig. 7 is the corresponding loci of contact points. It is easily seen that the loci of contact points of (V,F) contact is the line segment with tangent in the contact vertex deforming direction.

Remark. For the purpose of overlap checking, it suffices to use an arbitrary line segment with endpoints selected as interior point within *all* scaled polyhedron, instead of shortest path between inner ellipsoids. Setting

$$V_1^i = S_1, V_2^i = S_2,$$

and denoting

$$V_1 = v_{s_1}, V_2 = v_{s_2}, t_1 = t_{s_1}, t_2 = t_{s_2},$$

which are scaled to

$$\tilde{V}_{s_1} = \rho_1 V_{s_1}, \tilde{V}_{s_2} = \rho_2 V_{s_2} \text{ where}$$

$$v_{s_1} = t_{s_1} (s_2 - s_1), v_{s_2} = t_{s_2} (s_1 - s_2).$$

Then

$$\tilde{t}_{s_1} = \rho_1 t_{s_1}, \tilde{t}_{s_2} = \rho_2 t_{s_2}.$$

Thus, the mapping to $\tilde{t}_{s_1}, \tilde{t}_{s_2}$ is linearly related via

$$\tilde{t}_{s_2} = \tilde{a} \tilde{t}_{s_1} + \tilde{b}, \tilde{a} = \frac{t_{s_2}}{t_{s_1}} a, \tilde{b} = t_{s_2} b$$

since (ρ_1, ρ_2) are linearly related via (2). However, the use of shortest path between inner ellipsoids offers additional information: an accurate estimate of separation/penetration distance between scaled convex polyhedral objects.

IV CONCLUSION

In this paper, we present an exact collision detection method for two convex polyhedral objects whose allowed deformation is uniform but arbitrary scaling of vertices within given upper and lower limits. Whether there are overlaps between scaled convex polyhedral objects is checked by reference to the descending piecewise linear curve characterizing the set of all (t_1, t_2) of contact configurations, which depends on the initial configuration of the objects. The loci of contact points for two convex polyhedra undergoing scaling transformation is a piecewise linear curve.

Acknowledgment

This work was supported by National Science Council of R.O.C. under contracts NSC 94-2212-E-001-001, NSC 95-2212-E-001-001.

APPENDIX: Proof of (2)

There are six contact configurations between two convex polyhedra (Fig. 8): vertex-vertex, vertex-edge, vertex-face, edge-edge, edge-face, and face-face. Some of the geometric manipulations in the following derivations could be found in [5].

Notations: for $i=1,2$

s_i the seed point of polyhedron i

ρ_i scaling of polyhedron i

c_i the contact point (vertex or projective point of s_i on contact edge) of polyhedron i ,

$c'_i = c_i + \rho_i \vec{d}_i$ scaled position of c_i ,

$\vec{d}_i = c_i - s_i$ the scaling direction of polyhedron i

$D(x, y) = \|x - y\|$, the distance between the entities x, y (a point or an edge, a face)

(i) (F,V) contact

Refer to Fig.9. Let a_1, a_2, a_3 be the three vertices of the contact face F_1 of polyhedron 1, \vec{n}_1 be its unit outward normal. Then

$F_1 = \vec{n}_1 \cdot (a - a_1) = n_{1x}x + n_{1y}y + n_{1z}z + d_{a1} = 0$, and the scaled face with a_1 scaled to $a'_1 = a_1 + D(F_1, F'_1)\vec{n}_1$ is

$F'_1 = \vec{n}_1 \cdot (a - a'_1) = 0$

$= n_{1x}x + n_{1y}y + n_{1z}z + d_{a1} \pm D(F_1, F'_1)$

where the “ \pm ” sign denotes expanding or shrinking of F_1 . We take the plus sign (i.e. polyhedron 1 enlarged) in the following derivation.

Note that

$D(F_1, F'_1) = (\rho_1 - 1)D(s_1, F_1)$

$\rho_1 = D(s_1, F'_1) / D(s_1, F_1)$, $\rho_2 = D(s_2, c'_2) / D(s_2, c_2) = t|\vec{d}_2| / D(s_2, c_2)$

By substituting c'_2 into F'_1 and rearrange the equation, we get

$c'_2 = \rho_2(c_2 - s_2) + s_2$, and c'_2 on the F'_1 when (F,V) contact, therefore

$n_{1x}c'_{2x} + n_{1y}c'_{2y} + n_{1z}c'_{2z} + d_{a1} = 0$, c'_2 and a'_1 could be rewritten by ρ_1, ρ_2

$\rho_2 \text{dot}(\vec{n}_1, (c_2 - s_2)) + (n_{1x}s_{2x} + n_{1y}s_{2y} + n_{1z}s_{2z}) = \rho_1 \times \text{dot}(\vec{n}_1, (a_1 - s_1)) + (n_{1x}s_{1x} + n_{1y}s_{1y} + n_{1z}s_{1z})$

$\rho_2 = \frac{\rho_1 \text{dot}(\vec{n}_1, (a_1 - s_1)) + (n_{1x}s_{1x} + n_{1y}s_{1y} + n_{1z}s_{1z}) - (n_{1x}s_{2x} + n_{1y}s_{2y} + n_{1z}s_{2z})}{\text{dot}(\vec{n}_1, (c_2 - s_2))}$

$$= \frac{\rho_1 \text{dot}(\vec{n}_1, (a_1 - s_1)) + \text{dot}(\vec{n}_1, (s_1 - s_2))}{\text{dot}(\vec{n}_1, (c_2 - s_2))} \quad (1)$$

Therefore ρ_1, ρ_2 are linearly related. Furthermore, the new contact point. $c'_2 = c_2 + \rho_2 \vec{d}_2$ is obtained. The loci of contact points is a line segment with tangent \vec{d}_2 .

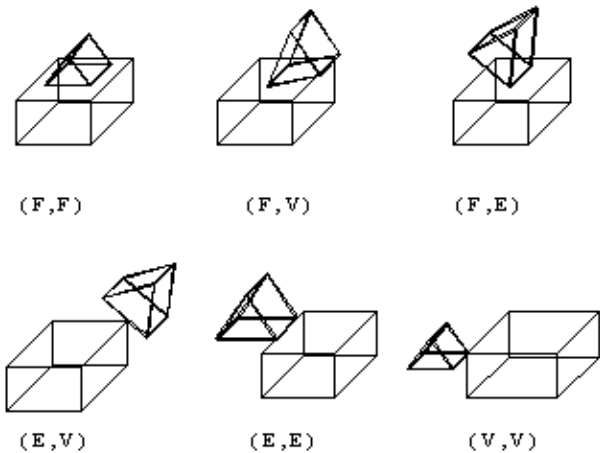


Fig. 8.Six contact features of two convex polyhedra contact externally

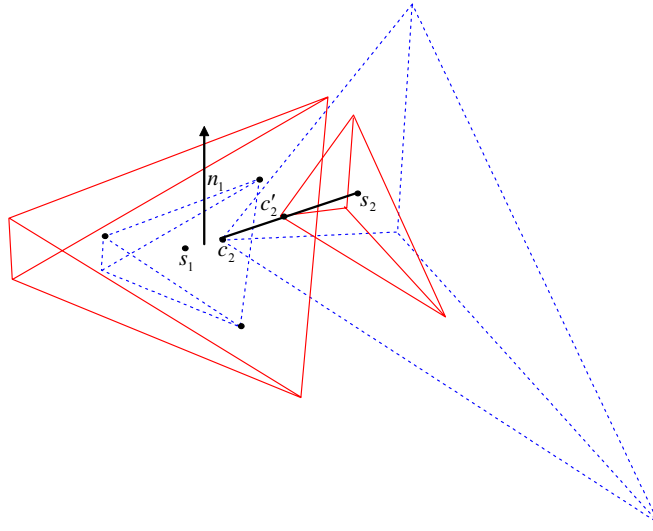


Fig. 9 (V,F) contact

(ii) (E,E) contact

Let v_{11}, v_{12} be end vertices of edge L_1 , v_{21}, v_{22} be the vertices of edge L_2 . Then

$$L_1(t) = v_{11} + t(v_{12} - v_{11}), t \in [0, 1]$$

$$L_2(s) = v_{21} + s(v_{22} - v_{21}), s \in [0, 1]$$

After scaling

$$L'_1(t) = v'_{11} + te'_1, e'_1 = v'_{12} - v'_{11}$$

$$L'_2(s) = v'_{21} + se'_2, e'_2 = v'_{22} - v'_{21}$$

L'_1, L'_2 intersect at one point, if there exist s, t , appropriate ρ_2 for given ρ_1 , $v'_{11} + te'_1 = v'_{21} + se'_2$, or

$$\underbrace{\begin{bmatrix} -(v_{12} - v_{11}) & v_{21} - s_2 & v_{22} - v_{21} \end{bmatrix}}_A \begin{bmatrix} t \\ \rho_2 \\ s\rho_2 \end{bmatrix}$$

$$= s_1 - s_2 + \rho_1(v_{11} - s_1)$$

If A is nonsingular, unique intersection exists, then we solve

$$\det[-(v_{12} - v_{11}), (s_1 - s_2) + \rho_1(v_{11} - s_1), (v_{22} - v_{21})] =$$

$$\det[-(v_{12} - v_{11}), (s_1 - s_2), (v_{22} - v_{21})] + \rho_1 \det[-(v_{12} - v_{11}), (v_{11} - s_1), (v_{22} - v_{21})]$$

$$\equiv \det[VS] + \rho_1 \det[VV]$$

$$\det[-(v_{12} - v_{11}), (v_{21} - s_2), (v_{22} - v_{21})] \equiv \det[A]$$

$$\rho_2 = \frac{\det[-(v_{12} - v_{11}), s_1 - s_2 + \rho_1(v_{11} - s_1), v_{22} - v_{21}]}{\det[-(v_{12} - v_{11}), (v_{21} - s_2), (v_{22} - v_{21})]} = \frac{\det[VS] + \rho_1 \det[VV]}{\det[A]} \quad (2)$$

which shows that ρ_1, ρ_2 are linearly related.

If $\det(A)=0$, and two edges $v_{12}-v_{11}, v_{22}-v_{21}$ are overlapping, there are an infinite of intersection points.

(iii) (V,E) contact as switching point where contact features change

(a) In most cases, the contact transition from (F,V) feature to (E,E) feature and vice versa is (V,E). In this situation,

$$\left\{ \begin{array}{l} \rho_2 = \frac{\rho_1 \text{dot}(\bar{n}_1, (a_1 - s_1)) + \text{dot}(\bar{n}_1, (s_1 - s_2))}{\text{dot}(\bar{n}_1, (c_2 - s_2))} \\ \rho_2 = \frac{\det[-\rho_1(v_{12} - v_{11}), s_1 - s_2 + \rho_1(v_{11} - s_1), v_{22} - v_{21}]}{\det[-\rho_1(v_{12} - v_{11}), v_{21} - s_2, v_{22} - v_{21}]} \end{array} \right. \text{Since } a_1 = v_{11}, L'_1, L'_2 \text{ intersect at } c'_2,$$

$$c'_2 = \rho_2(c_2 - s_2) + s_2 = v'_{11} + te'_1 = v'_{21} + se'_2$$

$$= \rho_1(v_{11} - s_1) + s_1 + t\rho_1(v_{12} - v_{11})$$

$$= \rho_2(v_{21} - s_2) + s_2 + s\rho_2(v_{22} - v_{21})$$

$$\rho_1 = \frac{\text{dot}(\bar{n}_1, (c_2 - s_2)) \det[VS] - \text{dot}(\bar{n}_1, (s_1 - s_2)) \det[A]}{\text{dot}(\bar{n}_1, (v_{11} - s_1)) \det[A] - \text{dot}(\bar{n}_1, (c_2 - s_2)) \det[VV]} \quad (3)$$

(b)(V,E) contact can also occur as the transition between (E,E) feature and (E,E) feature

As above

$$\left\{ \begin{array}{l} \rho_2 = \frac{\det[-\rho_1(v_{12} - v_{11}), s_1 - s_2 + \rho_1(v_{11} - s_1), v_{22} - v_{21}]}{\det[-\rho_1(v_{12} - v_{11}), v_{21} - s_2, v_{22} - v_{21}]} \\ \rho_2 = \frac{\det[-\rho_1(v_{12} - v_{11}), s_1 - s_2 + \rho_1(v_{11} - s_1), (v_{22} - v_{21})']}{\det[-\rho_1(v_{12} - v_{11}), (v_{21} - s_2)', (v_{22} - v_{21})']} \end{array} \right. \text{Equating the above equations yields}$$

$$\Rightarrow (\det[VS] + \rho_1 \det[VV]) \times \det[A'] = (\det[VS'] + \rho_1 \det[VV']) \times \det[A]$$

$$\rho_1 = \frac{\det[VS'] \times \det[A] - \det[VS] \times \det[A']}{\det[VV] \times \det[A'] - \det[VV'] \times \det[A]} \quad (4)$$

(c) (V,E) contact as transition between (F,V) feature and (F,V) feature

$$\left\{ \begin{array}{l} \rho_2 = \frac{\rho_1 \text{dot}(\bar{n}_1, (a_1 - s_1)) + \text{dot}(\bar{n}_1, (s_1 - s_2))}{\text{dot}(\bar{n}_1, (c_2 - s_2))} \\ \rho_2 = \frac{\rho_1 \text{dot}(\bar{n}'_1, (a_1 - s_1)') + \text{dot}(\bar{n}'_1, (s_1 - s_2)')}{\text{dot}(\bar{n}'_1, (c_2 - s_2))} \end{array} \right. \text{To} \quad (5)$$

$$\rho_1 = \frac{-\text{dot}(\bar{n}_1, (s_1 - s_2)) \text{dot}(\bar{n}'_1, (c_2 - s_2)) + \text{dot}(\bar{n}'_1, (s_1 - s_2)') \text{dot}(\bar{n}_1, (c_2 - s_2))}{\text{dot}(\bar{n}_1, (a_1 - s_1)) \text{dot}(\bar{n}'_1, (c_2 - s_2)) - \text{dot}(\bar{n}'_1, (a_1 - s_1)') \text{dot}(\bar{n}_1, (c_2 - s_2))}$$

(iv) (E,F) contact

Two situations occur in this case. One is that at least one vertex of contact edge is in the contact face. This situation can be reduced to (V,F) case by setting p_2 as the contact vertex. The other situation is that the two vertices of contact edge are outside the contact face. However, it does not influence the computation and linearity of ρ_1, ρ_2 . We only need to check whether the edge is still tangent to the face or not.

(v) (F,F) contact

Note that (F, F) contact occurs only when the pair of closest features are two parallel faces. This case can be reduced to (V,F) case by the following setting. Let p_2 , the projective point of s_2 onto the contact face of polyhedron 1, be the contact vertex and the unit normal \bar{n}_1 of the contact face of polyhedron 1 be the deforming direction of polyhedron 2. This might cause the deformed point p'_2 no longer located at F'_1 , but it does not influence the computation and linearity of ρ_1, ρ_2 . We only need to check whether the two faces are still tangent to each other or not.

(vi) (V,V) contact

To maintain a (V,V) contact under uniform scaling transformation, let a given contact vertex be $c_1 = c_2 = c$. The scaled contact vertex $c'_1 = c'_2$, or

$$s_1 + \rho_1(c_1 - s_1) = s_2 + \rho_2(c_2 - s_2) \quad (A1)$$

$$c = \frac{\rho_1 - 1}{\rho_1 - \rho_2} s_1 + \frac{1 - \rho_2}{\rho_1 - \rho_2} s_2$$

Thus $c \in s_1 s_2$, and if this is the case the contact scalings ρ_1, ρ_2 are linearly related via (A1). This could happen only for very special choice of seedpoints, rather than a generic contact case for scaled convex polyhedral objects.

From the linear relationship of touching scaling, it is easy to show that the scaled contact point of two called convex polyhedral objects has a linear relationship as well. For the cases of vertex-vertex, vertex-edge, and vertex-face contacts, the scaled contact point (vertex) is on the deforming direction. A linear relationship follows. Edge-face and face-face cases can be reduced to vertex-face case, so they also have a linear relationship. For edge-edge contact case, if we solve for the scaled contact point, we can find an equation showing the linear relationship between scaled contact point and ρ_1 . Therefore, scaled contact point of two designated convex polyhedral objects has a linear relationship for all six types of contact.

References

- [1] Gino van den Bergen, Collision detection in interactive 3D environments, Morgan Kaufmann Publishers, 2004.
- [2] P. Jimenez, F. Thomas, C. Torras, 3D collision detection: a survey, *Computer & Graphics*, vol.25, no. 2, pp.269-285, 2001.
- [3] M. Y. Ju, J.-S. Liu, S. P. Shiang, Y. R. Chien, K.S. Hwang, and W.C. Lee. Fast and accurate collision detection based on enclosed ellipsoid. *Robotica*, 19:381-394, 2001.
- [4] J.-S. Liu, J.I. Kao, YZ Chang, Collision detection of deformable polyhedral objects via inner-outer ellipsoids, *IEEE/RSJ Int. Conf. Intelligent Robots and Systems*, Beijing, China, Oct., 2006..
- [5] C. Ericson, Real-time collision detection, Elsevier, 2005.
- [6] T. Larsson and T. Akenine-Moller, Efficient collision detection for models deformed by morphing, *Visual Computer*, vol.19, pp.164-174, 2003
- [7] L. Kavan, J. Zara, Fast collision detection for skeletally deformable models, *Eurographics 2005*, vol.24, no.3.
- [8] Y. Kitamura, A. Smith, H. Takemura and F. Kishino, A real-time algorithm for accurate collision detection for deformable polyhedral objects, *Presence*, vol. 7, no. 1, pp.36-52, 1997.
- [9] E. Rimon and S. P. Boyd. Obstacle collision detection using best ellipsoid fit. *Journal of Intelligent and Robotic Systems*, 18:105-126, 1997.
- [10] C. Fares and Y. Hamam, Collision detection for rigid bodies: a state of the art review, *15th Int. Conf. Computer Graphics and Applications (GraphiCon'2005)*, Russia, June 2005.
- [11] W.Wang, Y.-K. Choi, B. Chan, M.-S. Kim and J. Wang, Efficient collision detection for moving ellipsoids using separating planes, *Computing* 72, pp.235-246, 2004.
- [12] M. Teschner, S. Kimmerle, B. Heidelberger et al. Collision detection for deforming objects, *Eurographics 2005*.
- [13] A. Akgunduz, P. Banerjee, and S. Mehrotra, A linear programming solution for exact collision detection. *Journal of Computing and Information Science in Engineering*, vol.5, pp.48-55, 2005.
- [14] K. Okada, M. Inaba, H. Inoue, Real-time and precise self collision detection system for humanoid robots, *2005 IEEE Int. Conf. Robotics and Automation*, pp.1072-1077, 2005.
- [15] Y.-K. Choi, X. Li, W. Wang, S. Cameron, Collision detection of convex polyhedra based on duality transformation, *Technical Report TR-2005-01*, Department of Computer Science, The University of Hong-Kong, 2005.
- [16] P. Jimenez, F. Thomas and C. Torras, Collision detection algorithms for motion planning, in J.-P. Latombe (Ed.): *Robot motion planning and control*, LNCIS 229, Ch6, 1998.
- [17] B.B. Goeree, E.D. Fasse and M.M. Marefat, Verifying contact hypotheses of planar polyhedral objects using penetration growth distance, *Robotics and Computer Integrated Manufacturing*, vol.17, pp.233-246, 2001.
- [18] S.A. Cameron and R.K. Culley, Determining the minimum translational distance between two convex polyhedra, *IEEE Int. Conf. Robotics and Automation*, pp.591-596, 1986.
- [19] S. Cameron, Enhancing GJK: Computing minimum and penetration distance between convex polyhedra, *IEEE Int. Conf. Robotics and Automation*, pp.3112-3117, 1997.
- [20] C.J. Ong and E.G. Gilbert, Growth distances: new measures for object separation and penetration, *IEEE Transaction on Robotics and Automation*, vol.12, no. 6, pp.888-903, 1996.
- [21] X. Zhu, H.Ding, S.K. Tso, A pseudodistance function and its applications, *IEEE Trans. Robotics and Automation*, vol.20. no.2, pp.344-352, 2004.
- [22] K. Forbes, Motion curves: a versatile representation for motion data, *M.S. Thesis*, Graduate Department of Computer Science, University of Toronto, 2005.
- [23] S.-M. Hong, J.-H. Yeo and H.-W. Park, A fast procedure for computing incremental growth distance, *Robotica*, vol.18, pp.429-441, 2000.